Absolute proton affinities of biphenyl and its derivatives

Zvonimir B. Maksić,*†[ab] Danijela Barić[a] and Borislav Kovačević[a]

[a] *Quantum Organic Chemistry Group, Rudjer Bošković Institute, PO Box 1016, 10000 Zagreb, Croatia*
[b] *Faculty of Science and Mathematics, The University of Zagreb, Marulićev trg 19, 10000 Zagreb, Croatia*

Received (in Cambridge) 2nd November 1998, Accepted 26th February 1999

The spatial structure of biphenyl **1** is studied by the semiempirical AM1 and *ab initio* HF/6-31G* and MP2(fc)/6-31G* theoretical models. The resulting bond distances are in good agreement with the X-ray structure. The calculated dihedral angle is in accordance with the value observed by the electron diffraction technique ($\varphi = 45°$). Its large value is a compromise between the steric hindrance effect and the π-electron conjugation. The estimated barrier heights for the internal rotation are very low however. Theoretical values are in accordance with the available experimental evidence. The calculated proton affinity (*PA*) obtained by the scaled $(AM1)_{sc}$ model and by using the MP2 level of theory compares very well with the experimental value. It is some 13 kcal mol^{-1} higher than the reference *PA* value of benzene, because of the strong resonance interaction between the two phenyl rings. The increase in the π-electron conjugation energy triggered by protonation overcomes the steric repulsion between H atoms thus decreasing the twist angle by some 20°. The apical carbon atom, placed *para* to the coannular CC bond, is most susceptible to the proton attack. On the other hand, the *PA* values for *ipso* and *meta* carbons are substantially lower since an amplification of the inter-ring conjugation interaction is then precluded. The *PA* increments for the CH_3 group and F atom monosubstituted biphenyls are determined by using the $(AM1)_{sc}$ approach. They are employed in estimating proton affinities of a number of polysubstituted biphenyls applying a very simple additivity formula based on the independent substituent approximation (ISA). It is shown that the performance of the additivity rule is very good. Variation in the *PA* of substituted biphenyls is rationalized in terms of the conjugation effect and repulsion between hydrogen atoms or substituents attached to the face-to-face *ortho* positions of the neighbouring rings (steric effect).

Finally, the proton affinity of fluorene possessing a "frozen" planar biphenyl moiety is calculated and compared with that of the paradigmatic Mills–Nixon (MN) system—indan. It is found that *PA* values of the former compound are determined by the MN and resonance effects, the latter being predominant. The most basic site in fluorene is the C(4) atom where both effects act in a synergistic way.

Introduction

Recently, a lot of attention has been focused on the relatively strong organic bases and especially on the so-called molecular proton sponges (PS). The paradigmatic 1,8-bis(dimethylamino)naphthalene (DMAN) proton sponge was discovered by Alder *et al.*[1] some thirty years ago. Relevant contributions to the field have been described in several review articles[2–5] and need not be discussed here. Resurrection of the interest in designing strong (super)bases is witnessed by numerous experimental[6–11] and theoretical[10–14] studies undertaken to shed light on their structure, stability and reactivity. Most of the studied highly basic systems were diamines. However, it was found that imines,[15] polyfunctional formamidines[16] and (a)cyclic guanidines[17] exhibit even higher basicities. The same holds for 2-alkylated tetrazenes.[18] We found that the imino group, attached to the quinoid-like six-membered ring, possesses high proton affinity (*PA*) due to the aromatization effect spurred by protonation.[19] By extending this concept to polycyclic quinoimines and quinodiimines we have been able to show that organic superbases could be constructed exhibiting *PA* values as high as 300 kcal mol^{-1} as a consequence of the aromatization spin-off effect.[20] In the present paper we examine the absolute proton affinity of biphenyl and its derivatives in order to get an insight into their gas phase basicities and propagation of the substituent effects across the system. This is of some interest since higher multiply substituted polyphenyls might be candidates for new materials exhibiting high basicity and/or important novel physical and chemical properties. A relation between the estimated *PA*s and the electronic features of biphenyls will be discussed, since the proton is a very good probe of the electronic structure of molecules. A particular emphasis will be laid on the propagation of the perturbation along the π-electron system induced by the protonation. The studied systems are depicted in Fig. 1.

Methodology

We have shown that the MP2(fc)/6-31G**//HF/6-31G*+ZPVE-(HF/6-31G*) *ab initio* model yields proton affinities in good agreement with the available experimental data for atoms of the first row elements,[21] nitrogen being a notable exception.[20] In this approach geometries are optimized at the HF/6-31G* level and the absolute minima on the energy hypersurface are confirmed by vibrational analysis. The accompanying vibrational frequencies are used to estimate the ΔZPVE contribution to the absolute proton affinity of the base in question by employing a common weighting factor, 0.89. ZPVE stands here for the zero-point vibrational energy as usual. The resulting total energies of bases and their conjugate acids are computed by the Möller–Plesset perturbation theory by taking into account energy correction of the second order. Also, a somewhat more flexible 6-31G** is utilized in the final calculation. This model will be denoted hereafter as MP2. It is gratifying, however, that much more economical models exist, which yield reasonable *PA* values being feasible in very large molecular systems. They are

† E-mail: zmaksic@spider.irb.hr; Fax: +385-1-4680-084.

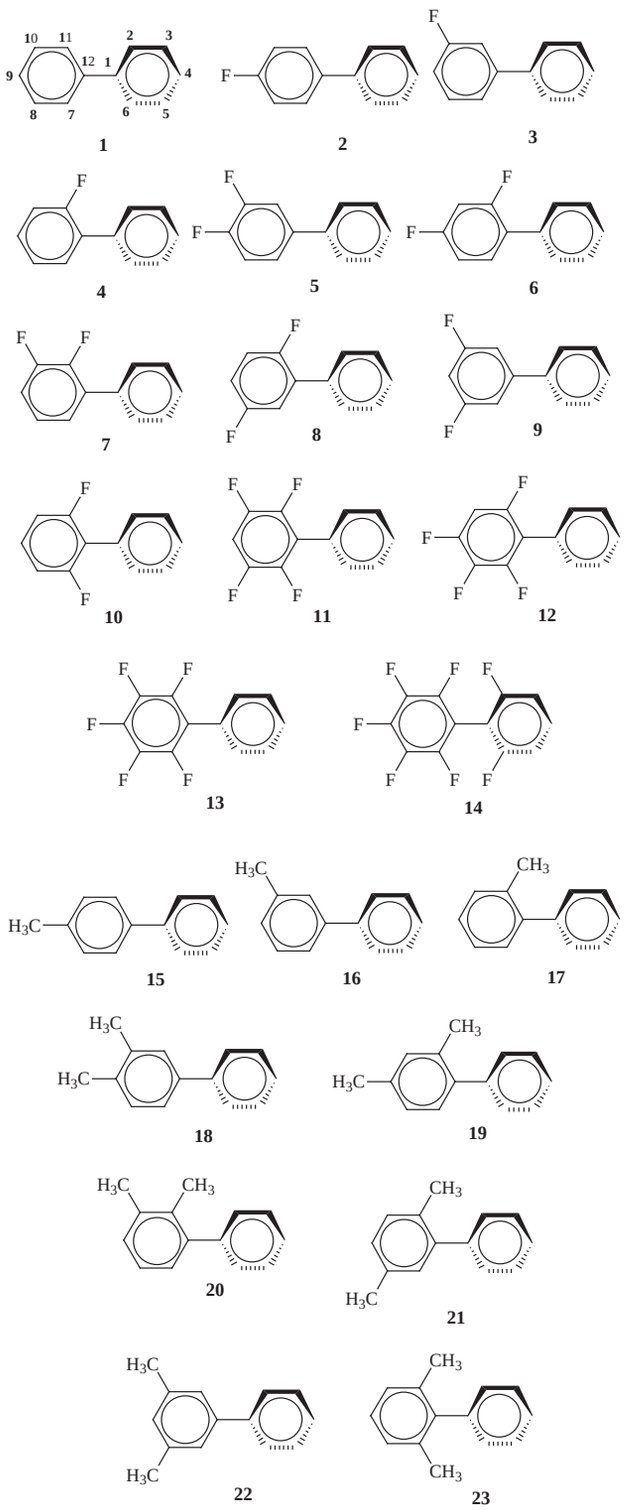

Fig. 1 Schematic representation and numbering of atoms of biphenyl and its derivatives.

based on an observation that (ΔZPVE) contributions to the proton affinity are fairly constant for atoms of the same element yielding *e.g.* the formula (1), where α denotes the

$$PA(\mathrm{MP2})_{\alpha} = 0.8633\ \Delta E_{\mathrm{el}}(\mathrm{HF/6\text{-}31G^*})_{\alpha} + 12.9 \quad (\mathrm{kcal\ mol^{-1}}) \quad (1)$$

attacked carbon atom of the aromatic ring and $\Delta E_{\mathrm{el}}(\mathrm{HF/6\text{-}31G^*})_{\alpha}$ stands for the difference in the Hartree–Fock energies between the examined base and its conjugate acid. A high quality of correlation is given by (1) for the scaled HF model.[22] Analogously, there is a good linear relationship between the MP2 proton affinities and AM1 heats of formation giving the semiempirical formula (2), where $\Delta H_{\mathrm{f}}^{\circ}$ represents the AM1 heats

$$PA(\mathrm{MP2})_{\alpha} = 1.2055[\Delta H_{\mathrm{f}}^{\circ}(\mathrm{B}) - \Delta H_{\mathrm{f}}^{\circ}(\mathrm{BH}_{\alpha}^{+})] + 404.3 \quad (\mathrm{kcal\ mol^{-1}}) \quad (2)$$

of formation of the species, stated between parentheses, in the gas phase.[22] In developing formula (2) use of the $\Delta H_{\mathrm{f}}^{\circ}(\mathrm{H}^{+})$ value for the proton of 367.2 kcal mol^{-1} was made. This semiempirical model will be denoted as $(\mathrm{AM1})_{\mathrm{sc}}$ and referred to as the scaled AM1 approach. We shall employ it here rather heavily because of the large number of calculations required for *PA*s of sizeable substituted biphenyl systems. However, the $(\mathrm{AM1})_{\mathrm{sc}}$ model will be tested first for the parent biphenyl system against more accurate methods and some available experimental data.

Results and discussion

Spatial structures

Geometries of biphenyl **1** and its protonated forms obtained by AM1, HF/6-31G* and MP2(fc)/6-31G* theoretical models are given in Table 1. The crystal structure parameters[23] are available for the parent system **1**. Perusal of the presented results shows that *ab initio* bond lengths are in very good agreement with experiment. The semiempirical AM1 estimates are in reasonable accordance with more accurate data provided by more rigorous methods and experimental measurements. In particular, variation in bond distances is reproduced correctly. Hence, one concludes that the AM1 scheme is well suited for studying the biphenyl family of compounds. This conclusion is strengthened by the AM1 *PA* value, which is also in good accordance with the MP2 result and experiment (*vide infra*). As a final comment on the structure of **1** we note that the dihedral (twist) angle of two phenyl planes is 40.6, 45.5 and 44.6° by the AM1, HF/6-31G* and MP2(fc)/6-31G* models, respectively, which is in agreement with the gas phase electron diffraction estimate (ED)[24] of 45°. Such a large twist angle is a compromise between the steric repulsion of hydrogen atoms attached to *ortho* carbons and the delocalization effect across the central bond. It is interesting to mention that the barrier for the internal rotation is rather low. It has two maxima corresponding to the twist angles $\varphi = 0°$ (2.1; 3.3; 4.0 kcal mol^{-1}), and $\varphi = 90°$ (1.0; 1.5; 1.8 kcal mol^{-1}), where triplets of numbers given within parentheses correspond to results of the AM1, HF/6-31G* and MP2(fc)/6-31G* models, respectively. In this connection it is noteworthy that the crystal structure of **1** is planar, apparently due to the intermolecular interactions.[23] In solutions biphenyl has twisted planes by some 15–30° as evidenced by spectroscopic studies.[25–28] These results indicate that biphenyl is a low barrier molecular rotor as a consequence of a subtle balance between the resonance and steric effects. This finding is not surprising since the delocalization effect is rather weak as evidenced by a comparison of the π-bond orders of biphenyl and *trans*-buta-1,3-diene. They are 0.28 (0.27) and 0.25 (0.31), respectively, as obtained by the AM1 (HF/6-31G*) models. It follows that delocalization of π-electrons in biphenyl is similar to that found in the well localized buta-1,3-diene system. A comparison with the experimental barrier heights is in place here. The ED data[24] are consistent with the identical maxima of the internal rotation potential which read $V_0 = 1.4 \pm 0.5$ and $V_{90} = 1.6 \pm 0.5$ for the planar and perpendicular conformation, respectively. Theoretical results indicate that the upper limit of V_0 should be taken as a more realistic estimate of the overall maximum, whereas the experimental value $V_{90} = 1.6$ kcal mol^{-1} is in good agreement with all three theoretical models. We note in passing that the height of the torsional potential changes in the solution, but not to a dramatic extent. For example, the spin-lattice relaxation measurement of perdeuterobiphenyl is

Table 1 Selected structural parameters of biphenyl (**1**) and its protonated forms as offered by several theoretical models and crystallographic data (in Å)

Molecule	Bond	AM1	HF/6-31G*	MP2(fc)/6-31G*
1	C(1)–C(2)	1.402	1.393	1.404 [1.395(3)][a]
	C(2)–C(3)	1.393	1.385	1.395 [1.392(4)]
	C(3)–C(4)	1.395	1.385	1.397 [1.388(4)]
	C(1)–C(12)	1.461	1.491	1.478 [1.493(3)]
$\mathbf{1}_1$	C(1)–C(2)	1.478	1.484	1.465
	C(2)–C(3)	1.373	1.354	1.376
	C(3)–C(4)	1.408	1.409	1.409
	C(4)–C(5)	1.408	1.409	1.409
	C(5)–C(6)	1.373	1.354	1.376
	C(6)–C(1)	1.478	1.484	1.465
	C(7)–C(12)	1.399	1.391	1.399
	C(7)–C(8)	1.395	1.383	1.395
	C(11)–C(12)	1.400	1.386	1.397
	C(10)–C(11)	1.394	1.387	1.397
	C(8)–C(9)	1.395	1.387	1.398
	C(1)–C(12)	1.502	1.537	1.568
$\mathbf{1}_2$	C(1)–C(2)	1.482	1.499	1.486
	C(2)–C(3)	1.472	1.487	1.475
	C(3)–C(4)	1.360	1.336	1.366
	C(4)–C(5)	1.422	1.429	1.419
	C(5)–C(6)	1.385	1.377	1.392
	C(6)–C(1)	1.404	1.392	1.400
	C(7)–C(12)	1.414	1.405	1.415
	C(7)–C(8)	1.390	1.378	1.390
	C(11)–C(12)	1.416	1.405	1.414
	C(10)–C(11)	1.387	1.377	1.390
	C(8)–C(9)	1.396	1.387	1.400
	C(1)–C(12)	1.434	1.453	1.445
$\mathbf{1}_3$	C(1)–C(2)	1.382	1.359	1.389
	C(2)–C(3)	1.464	1.477	1.464
	C(3)–C(4)	1.466	1.475	1.464
	C(4)–C(5)	1.372	1.351	1.376
	C(5)–C(6)	1.408	1.411	1.409
	C(6)–C(1)	1.416	1.417	1.416
	C(7)–C(12)	1.403	1.391	1.404
	C(7)–C(8)	1.393	1.384	1.394
	C(11)–C(12)	1.402	1.391	1.403
	C(10)–C(11)	1.393	1.384	1.394
	C(8)–C(9)	1.396	1.386	1.398
	C(1)–C(12)	1.461	1.491	1.472
$\mathbf{1}_4$	C(1)–C(2)	1.430	1.437	1.430
	C(2)–C(3)	1.361	1.341	1.365
	C(3)–C(4)	1.471	1.481	1.473
	C(7)–C(12)	1.415	1.407	1.416
	C(7)–C(8)	1.389	1.377	1.389
	C(8)–C(9)	1.398	1.389	1.400
	C(1)–C(12)	1.433	1.446	1.441

[a] X-Ray structure of ref. 23.

3.5 kcal mol^{-1} [29] in dimethyl sulfoxide. It appears that the barrier of rotation of the biphenyl framework remains persistently low in very different environments. This situation is quite different in its protonated forms (*vide infra*). It is of some interest to develop the potential $V(\varphi)$ of the hindered rotation in the Fourier series truncated after the fourth nonvanishing term [eqn. (3)].

$$V(\varphi) = C_0 + C_2(1 - \cos 2\varphi) + C_4(1 - \cos 4\varphi) + C_6(1 - \cos 6\varphi) \quad (3)$$

The least squares fit for the AM1 ΔH_f° values yields the following numerical values: $C_0 = 2.1$, $C_2 = -0.2$, $C_4 = -0.7$ and $C_6 = -0.3$. The average absolute error is 0.2 kcal mol^{-1} whereas the correlation coefficient is 0.75. The latter is small because the torsional potential is very low. The protonated species exhibit some interesting structural features, which are best illustrated by the resonance structures depicted in Scheme 1.

A striking detail in Scheme 1 is the fact that the positive charge ("an empty π-orbital") occurs at the central bridge bond for *ortho* and *para* protonation in $\mathbf{1}_2$ and $\mathbf{1}_4$, respectively, thus

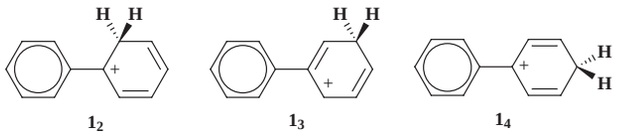

Scheme 1

enabling additional delocalization of the positive charge within the neighbouring benzene moiety. This is represented by the resonance structures shown in Scheme 2 for the *para* protonation case.

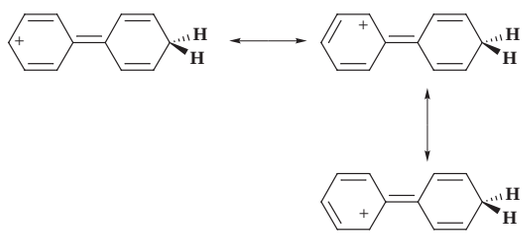

Scheme 2

Obviously, there is an increase in the double bond character of the coannular C(1)–C(12) bond and an increased bond localization in the unprotonated phenyl ring. The same should hold for the *ortho* protonation. The AM1 π-bond orders corroborate this conjecture as evidenced by their values 0.16, 0.45 and 0.42 in **1**, $\mathbf{1}_2$ and $\mathbf{1}_4$ respectively. In contrast, the π-bond order of the C(1)–C(12) bond in $\mathbf{1}_3$ is 0.17 since conjugation described by Scheme 2 is impossible for the *meta* protonation. If the picture offered by bond lengths is correct, then the twist angles in $\mathbf{1}_2$ and $\mathbf{1}_4$ should be considerably smaller than in the parent compound, whereas it should be roughly the same in $\mathbf{1}_3$ as in the initial base. This is indeed the case. The twist angles φ in **1**, $\mathbf{1}_2$, $\mathbf{1}_3$ and $\mathbf{1}_4$ are 40.6, 14.2, 42.4 and 23.7°, respectively. It is interesting that the dihedral angle φ differs for *ortho* and *para* protonation. A plausible explanation is given by the fact that the former species involves formation of the sp^3 centre in the vicinity of a repulsive *ortho* hydrogen atom of the neighbouring ring. Hence, this H atom is better placed within the created H–C–H scissors thus decreasing the nonbonded interactions. Concomitantly, the twist angle is smaller for *ortho* attack ($\varphi = 14.2°$). Bond distances of the coannular central CC bond are in harmony with the presented analysis. They are shortened in the $\mathbf{1}_2$ and $\mathbf{1}_4$ protonated species relative to the parent system **1** by some 0.03–0.04 Å depending on the theoretical model used. In contrast, this bond length remains virtually unchanged in $\mathbf{1}_3$. Finally, the barrier of rotation should be increased in systems $\mathbf{1}_2$ and $\mathbf{1}_4$. AM1 calculation shows that in the latter conjugate acid the ΔH_f° value for the perpendicular conformation ($\varphi = 90°$) is increased by 6 kcal mol^{-1} relative to the equilibrium ($\varphi = 23.7°$) ΔH_f° value of 221.4 kcal mol^{-1}. The coplanar configuration is only 0.6 kcal mol^{-1} less stable than the equilibrium distribution of atoms. These data are in harmony with the increased resonance interaction in $\mathbf{1}_4$. The internal rotation potential for the *para* protonated biphenyl estimated by the AM1 model is given by eqn. (4).

$$V(\varphi)_P^+ = 0.1 + 3.1(1 - \cos 2\varphi) + (-1.0)(1 - \cos 4\varphi) + (-0.1)(1 - \cos 6\varphi) \quad (4)$$

The average absolute error is 0.3 kcal mol^{-1} whereas the correlation coefficient is 0.98. The quality of the correlation is much better for the protonated species than in the case of the parent biphenyl, because the barrier height is substantially higher.

Proton affinities of benzene and biphenyl

The *PA* values of **1** and benzene estimated by several theoretical

models are compared with the experimental data in Table 2. It appears that the $(AM1)_{sc}$ model gives excellent agreement with experiment for **1**, which offers additional support to the semiempirical approach adopted here. The *para* position is most susceptible to proton attack as intuitively expected. It is interesting to note that the *PA* of **1** is some 13 kcal mol^{-1} higher than that of benzene. This is a consequence of the larger resonance effect in conjugate acids $\mathbf{1}_2$ and $\mathbf{1}_4$ being concomitant with a more favourable distribution of the positive charge over the whole molecular system as discussed earlier. On the other hand the relaxation effect propagates through the σ-framework rather inefficiently as evidenced by the slightly increased *PA* value in $\mathbf{1}_3$ by some 3 kcal mol^{-1} relative to benzene. This example illustrates nicely the importance of the mobile π-electrons in transmitting chemical information along the extended π-systems.

The effect of substituents on the proton affinity

The change in the *PA* of monosubstituted aromatics relative to the unsubstituted parent compounds is embodied in the corresponding increments, which are discussed in great detail elsewhere.[21,31–33] In the present paper we examine the influence of F and CH_3 substituents on the proton affinity of mono- and polysubstituted biphenyls with a particular emphasis on the additivity effect in the multiply substituted compounds. The increments $I^+(X_\beta)_\alpha$, where indices α and β denote positions of the proton and substituent, respectively, while *X* stands for F and the CH_3 group, are given in Table 3. It should be mentioned that *ipso* protonation is not considered here because it requires a separate treatment as far as the additivity is concerned.[34] A survey of the results presented in Table 3 shows that fluorine deactivates all positions in biphenyls **2**–**4**. This is apparently a consequence of the strong σ-electron withdrawing property of the highly electronegative fluorine atom. The lowest increments are found at *meta* positions measured relative to the fluorine substitution site. It appears, namely, that other positions are somewhat stabilized *via* the π-electron back bonding effect of fluorine. This holds both for the substituted and the neighbouring phenyl ring except in **3**, where π-back bonding conjugation with the second ring is precluded by the *meta* fluorine position relative to the central CC bond. This conclusion can be easily verified by examining the relevant canonical resonance structures. Consequently, increments for the neighbouring ring in the protonated species of the isomer **3** are lower than in **2**. The increments in **4** reflect the interplay between the resonance effect and repulsion between F and H atoms placed at face-to-face *ortho* positions.

The methyl group is a well known σ- and π-electron density donor. It is, therefore, not surprising that it activates practically all positions in molecules **15** and **16**. Again, the increments for the nonsubstituted phenyl ring in **16** are lower than in **15**, since propagation of the hyperconjugative interaction to the second ring in the former molecule is precluded by the unfavourable CH_3 (*meta* substitution) position. This example shows clearly that if the enhanced proton affinity of the aromatic systems is desired, then one needs the right substituent(s) placed at the right position(s). This is in harmony with our earlier results obtained in studying proton affinity and in designing strong organic bases.[19,20] Finally, negative increments occurring in **17** are a consequence of the interference of the bulky CH_3 group with the H atom of the neighbouring ring.

Table 2 The proton affinities of benzene and biphenyl (in kcal mol^{-1})[a]

Conjugate acid	AM1	HF/ 6-31G*	MP2(fc)// HF/6-31G*	MP2(fc)/ 6-31G*	Exp.[b]
Benzene–H^+	182.6	189.4	179.9	177.5	179.9
$\mathbf{1}_1$	178.3	187.7	177.7	175.4	—
$\mathbf{1}_2$	193.2	199.6	190.5	188.1	—
$\mathbf{1}_3$	185.5	192.0	183.3	181.1	—
$\mathbf{1}_4$	194.8	202.6	192.8	190.1	194.5

[a] The single point MP2(fc) calculations were carried out using the 6-31G** basis set. [b] Experimental results of ref. 30.

Table 3 The proton affinity and its increments in monosubstituted fluoro- and methylbiphenyls as obtained by the $(AM1)_{sc}$ model (in kcal mol^{-1})[a]

Conjugate acid	φ(BH^+)/°	*PA*	$I^+(F_\beta)_\alpha$	Conjugate acid	φ(BH^+)/°	*PA*	$I^+[(CH_3)_\beta]_\alpha$
$\mathbf{2}_1$	65.4	175.1	−3.2	$\mathbf{15}_1$	65.4	179.2	0.9
$\mathbf{2}_2$	19.4	190.6	−2.6	$\mathbf{15}_2$	7.4	195.5	2.3
$\mathbf{2}_3$	42.5	182.7	−2.8	$\mathbf{15}_3$	41.4	186.5	1.0
$\mathbf{2}_4$	22.4	192.4	−2.4	$\mathbf{15}_4$	21.4	197.1	2.3
$\mathbf{2}_7$	10.5	185.1	−8.1	$\mathbf{15}_7$	14.1	194.4	1.2
$\mathbf{2}_8$	42.1	184.1	−1.4	$\mathbf{15}_8$	42.1	190.7	5.2
$\mathbf{2}_{12}$	65.4	178.3	0.0	$\mathbf{15}_{12}$	63.9	182.6	4.3
$\mathbf{3}_1$	65.4	175.0	−3.3	$\mathbf{16}_1$	65.4	179.2	0.9
$\mathbf{3}_2$	18.5	188.5	−4.7	$\mathbf{16}_2$	13.8	194.0	0.8
$\mathbf{3}_3$	43.3	182.5	−3.0	$\mathbf{16}_3$	42.4	186.2	0.7
$\mathbf{3}_4$	26.0	190.0	−4.8	$\mathbf{16}_4$	23.8	195.6	0.8
$\mathbf{3}_5$	43.3	182.4	−3.1	$\mathbf{16}_5$	42.5	186.2	0.7
$\mathbf{3}_6$	20.3	188.3	−4.9	$\mathbf{16}_6$	14.4	194.0	0.8
$\mathbf{3}_7$	15.7	192.5	−0.7	$\mathbf{16}_7$	18.6	198.3	5.1
$\mathbf{3}_8$	42.0	176.3	−9.2	$\mathbf{16}_8$	42.8	187.0	1.5
$\mathbf{3}_9$	24.1	193.3	−1.5	$\mathbf{16}_9$	25.5	198.8	4.0
$\mathbf{3}_{11}$	15.6	191.0	−2.2	$\mathbf{16}_{11}$	18.2	196.9	3.7
$\mathbf{3}_{12}$	53.7	168.7	−9.6	$\mathbf{16}_{12}$	60.8	179.7	1.4
$\mathbf{4}_1$	66.0	176.7	−1.6	$\mathbf{17}_1$	66.4	178.9	0.6
$\mathbf{4}_2$	18.3	192.4	−0.8	$\mathbf{17}_2$	33.1	191.5	−2.3
$\mathbf{4}_3$	43.9	185.6	0.1	$\mathbf{17}_3$	51.5	186.3	0.8
$\mathbf{4}_4$	29.6	193.0	−1.8	$\mathbf{17}_4$	36.6	194.4	−0.4
$\mathbf{4}_5$	45.3	185.4	−0.1	$\mathbf{17}_5$	52.4	186.4	0.9
$\mathbf{4}_6$	18.3	191.0	−2.2	$\mathbf{17}_6$	40.8	192.5	−0.7
$\mathbf{4}_7$	23.4	184.2	−9.0	$\mathbf{17}_7$	43.5	192.5	−0.7
$\mathbf{4}_8$	48.3	185.7	0.2	$\mathbf{17}_8$	58.6	192.1	6.6
$\mathbf{4}_9$	28.4	186.1	−8.7	$\mathbf{17}_9$	38.5	193.8	−1.0
$\mathbf{4}_{10}$	47.7	184.6	−0.7	$\mathbf{17}_{10}$	72.8	191.1	5.6
$\mathbf{4}_{12}$	53.3	178.9	0.6	$\mathbf{17}_{12}$	77.8	184.9	6.6

[a] The twist angle in conjugate acids is denoted by φ(BH^+) and given in degrees. The dihedral angles of initial bases are as follows: φ(**2**) = 40.7°, φ(**3**) = 40.8°, φ(**4**) = 45.0°, φ(**15**) = 40.3°, φ(**16**) = 40.8° and φ(**17**) = 53.3°.

Table 4 The proton affinity of some polyfluoro- and polymethylbiphenyls obtained by the $(AM1)_{sc}$ model and the additivity rule based on the independent substitution approximation (in kcal mol^{-1})[a]

Conjugate acid	$\varphi(BH^+)$/°	*PA*	PA_{ad}	Conjugate acid	$\varphi(BH^+)$/°	*PA*	PA_{ad}
$\mathbf{5}_2$	15.0	186.0	185.9	$\mathbf{18}_2$	7.6	196.2	196.3
$\mathbf{5}_3$	43.5	179.7	179.7	$\mathbf{18}_3$	41.6	187.1	187.2
$\mathbf{5}_4$	24.8	187.7	187.6	$\mathbf{18}_4$	21.6	197.8	197.9
$\mathbf{5}_5$	43.5	179.7	179.6	$\mathbf{18}_5$	41.5	187.1	187.2
$\mathbf{5}_6$	16.8	185.8	185.7	$\mathbf{18}_6$	8.4	196.2	196.3
$\mathbf{5}_7$	12.7	184.6	184.4	$\mathbf{18}_7$	18.9	199.1	199.5
$\mathbf{5}_8$	41.9	175.1	174.9	$\mathbf{18}_8$	42.6	192.0	192.2
$\mathbf{5}_{11}$	11.8	183.2	182.9	$\mathbf{18}_{11}$	18.2	198.0	198.1
$\mathbf{6}_2$	17.1	189.7	189.8	$\mathbf{19}_2$	29.4	193.6	193.2
$\mathbf{6}_3$	44.3	182.8	182.8	$\mathbf{19}_3$	50.9	187.2	187.3
$\mathbf{6}_4$	28.9	190.5	190.6	$\mathbf{19}_4$	35.1	196.3	196.7
$\mathbf{6}_5$	45.2	182.6	182.6	$\mathbf{19}_5$	50.5	187.3	187.4
$\mathbf{6}_6$	23.8	188.4	188.4	$\mathbf{19}_6$	37.7	194.4	194.8
$\mathbf{6}_7$	20.7	176.2	176.1	$\mathbf{19}_7$	43.1	193.7	193.7
$\mathbf{6}_8$	48.3	183.8	184.3	$\mathbf{19}_8$	74.8	196.8	197.3
$\mathbf{6}_{10}$	47.0	182.5	183.4	$\mathbf{19}_{10}$	70.8	195.6	196.3
$\mathbf{7}_2$	22.0	187.8	187.7	$\mathbf{20}_2$	51.7	191.8	191.7
$\mathbf{7}_3$	44.8	182.5	182.5	$\mathbf{20}_3$	53.6	187.0	187.0
$\mathbf{7}_4$	32.2	188.4	188.2	$\mathbf{20}_4$	38.9	194.9	195.2
$\mathbf{7}_5$	45.8	182.3	182.0	$\mathbf{20}_5$	53.9	187.1	187.1
$\mathbf{7}_6$	32.2	186.4	186.1	$\mathbf{20}_6$	43.0	193.1	193.3
$\mathbf{7}_8$	48.3	176.9	176.5	$\mathbf{20}_8$	74.7	193.3	193.6
$\mathbf{7}_9$	28.8	185.0	184.6	$\mathbf{20}_9$	40.7	197.9	197.8
$\mathbf{8}_2$	22.0	187.7	187.5	$\mathbf{21}_2$	32.8	192.3	191.7
$\mathbf{8}_3$	44.4	182.5	182.5	$\mathbf{21}_3$	50.2	187.0	187.0
$\mathbf{8}_4$	32.0	188.5	188.2	$\mathbf{21}_4$	38.0	195.1	195.2
$\mathbf{8}_5$	45.2	182.4	182.4	$\mathbf{21}_5$	51.0	187.1	187.1
$\mathbf{8}_6$	29.6	186.7	186.3	$\mathbf{21}_6$	31.1	192.4	192.3
$\mathbf{8}_7$	25.1	182.4	182.0	$\mathbf{21}_7$	45.3	196.6	196.2
$\mathbf{8}_9$	30.0	184.9	184.6	$\mathbf{21}_9$	42.0	197.9	197.9
$\mathbf{8}_{10}$	47.8	176.1	175.6	$\mathbf{21}_{10}$	71.8	192.5	192.6
$\mathbf{9}_2$	25.2	183.9	183.6	$\mathbf{22}_2$	14.1	194.9	194.8
$\mathbf{9}_3$	44.1	179.5	179.4	$\mathbf{22}_3$	42.6	186.9	187.1
$\mathbf{9}_4$	28.4	185.5	185.2	$\mathbf{22}_4$	23.3	196.4	196.4
$\mathbf{9}_7$	17.2	190.1	190.3	$\mathbf{22}_7$	22.0	201.8	202.0
$\mathbf{9}_9$	24.2	191.1	191.8	$\mathbf{22}_9$	27.0	202.4	202.8
$\mathbf{10}_2$	34.2	189.9	190.2	$\mathbf{23}_2$	60.6	191.0	190.2
$\mathbf{10}_3$	47.3	185.6	185.5	$\mathbf{23}_3$	75.5	186.8	187.2
$\mathbf{10}_4$	36.4	191.1	191.2	$\mathbf{23}_4$	47.2	193.3	194.0
$\mathbf{10}_8$	34.0	177.3	177.4	$\mathbf{23}_8$	80.7	197.4	197.7
$\mathbf{10}_9$	55.4	184.7	185.0	$\mathbf{23}_9$	50.9	192.8	192.8
$\mathbf{11}_2$	44.3	181.9	180.6	$\mathbf{14}_3$	90.0	176.4	176.1
$\mathbf{11}_3$	48.2	179.7	179.4	$\mathbf{14}_4$	44.6	160.9	161.8
$\mathbf{11}_4$	39.6	182.7	181.6				
$\mathbf{11}_9$	34.6	175.0	174.4				

[a] The twist angle in conjugate acids is denoted by $\varphi(BH^+)$ and given in degrees. The dihedral angles of initial bases are as follows: φ(**5**) = 40.8°, φ(**6**) = 44.1°, φ(**7**) = 44.2°, φ(**8**) = 45.1°, φ(**9**) = 40.9°, φ(**10**) = 49.3°, φ(**11**) = 49.6°, φ(**18**) = 40.4°, φ(**19**) = 51.4°, φ(**20**) = 56.4°, φ(**21**) = 53.3°, φ(**22**) = 41.0°, φ(**23**) = 78.6 and φ(**14**) = 90.0°.

Polysubstituted biphenyls

There is a simple additivity rule based on the independent substituent approximation (ISA), which yields good estimates of the *PA* values in heavily substituted aromatics.[21,31–34] Briefly, the proton affinity in polysubstituted biphenyls should be approximately given by the *PA* value of the unsubstituted parent biphenyl system and a sum of the corresponding increments [eqn. (5)], where summation is extended over all substituents *X*,

$$PA(\text{subst. biphenyl})_\alpha = PA(\text{biphenyl}) + \sum_{X_\beta} I^+(X_\beta)_\alpha \quad (5)$$

whilst α is the site of the protonation. Employing the incremental contributions for F and CH_3 substituents presented in Table 3 one can easily derive the *PA* values of polysubstituted biphenyls **5**–**14** and **18**–**23**. They are tested against the $(AM1)_{sc}$ results in Table 4. One observes that the elementary additivity rule performs very well since the differences from results offered by the scaled AM1 model are practically negligible. The dihedral twist angles of the initial bases and the resulting conjugate acids are presented in Table 4 too. They give a direct insight into the degree of the π-electron conjugation. Although presented data speak for themselves, it is interesting to point out that two methyl groups in **23** give rise to a large twist angle φ(B) of 78.6°. This angle is diminished to significantly lower values if the proton is attached to the C atom in such a way that it triggers substantial π-conjugation. Another striking case is provided by the heavily fluorinated biphenyl **14**, where phenyl rings are perpendicular due to a strong vicinal repulsion of four F atoms. Protonation at the C(3) atom leaves the right φ(B) = 90° angle unchanged, but proton attack at the apical C(4) atom decreases the twist angle by 45°, which is in accordance with the increased π-electron conjugation.

The protonation of fluorene and the Mills–Nixon Effect

The π-electron conjugation is a maximum if the dihedral twist angle φ in biphenyl vanishes. This conformation cannot be realized in practice because of steric hindrance. There are, however, molecular systems which do involve the "frozen" planar biphenyl framework. The simplest case is provided by fluorene **24** depicted in Fig. 2. This compound will be con-

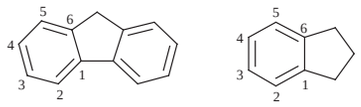

24 25

Fig. 2 The dominant resonance structure of fluorene **24** and indan **25**.

sidered here in the context of the much debated Mills–Nixon effect.[35] We have conclusively shown that fusion of a small ring to an aromatic moiety leads to substantial changes of a large number of physical and chemical properties of the aromatic fragment including its reactivity.[36] The most recent contribution to the field involving an extensive list of the relevant literature was given by Kochi *et al*.[37] The paradigmatic MN system is provided by indan **25** (Fig. 2). It is well known by now that rehybridization at the carbon junction atoms leads to a partial π-electron localization as shown in Fig. 2. This leads to regioselectivity in the electrophilic substitution reactions, which can be rationalized by competition of two localization patterns—one occurring in the initial ground state of a reactant (the memory effect) and the other taking place in the transition structure (TS) mimicked by Wheland intermediates.[38–40] It appears that a degree of this mismatching is smaller for the β than for the α position. Consequently, the α-position is significantly disfavoured thus making the β-position in **25** more susceptible toward electrophilic attack. This is in harmony with the experimental evidence.[35] Since the proton is the simplest electrophilic particle, it follows that *PA*(C(3)) should be higher than *PA*(C(2)). This is indeed the case as evidenced by the $(AM1)_{sc}$ calculations (Table 5). It is interesting to compare the proton affinities of fluorene **24** with those of the archetypal indan **25**. We note first that fluorene exhibits partial π-bond fixation as indicated in Fig. 2, which in turn is caused by rehybridization. This is in accordance with Brown's early postulate that *exo* double bonds stabilize a five-membered ring.[41] It would appear at first sight that both β-positions should be energetically more favourable for the protonation according to the MN hypothesis. The situation is more complex as evidenced by results presented in Table 5. The hierarchy of the *PA* values reads: $PA(\mathbf{24_4}) > PA(\mathbf{24_2}) > PA(\mathbf{24_3}) > PA(\mathbf{24_5})$ indicating that the propensity to protonation is the highest for the β-site C(4) as intuitively expected. However, the second largest proton affinity is related to the α-position C(2) showing that another intramolecular interaction overshadows the MN effect. This can be identified as the conjugation across the planar biphenyl framework triggered by protonation at the *para* and *ortho* carbons relative to the C(1) atom. Moreover, by comparison with the corresponding *PA* values of indan one concludes that an increase in the π-electron delocalization upon protonation at *para* and *ortho* carbon atoms is roughly equal, being approximately 7 kcal mol^{-1} in both cases. Hence, the difference in $PA(\mathbf{24_4})$ and $PA(\mathbf{24_2})$ of 2.7 kcal mol^{-1} can be ascribed to the MN effect. A slightly lower estimate is obtained by comparing $PA(\mathbf{24_3})$ and $PA(\mathbf{24_5})$ for the proton attacks, which do not induce additional resonance as discussed earlier (*vide supra*). This difference is 1.9 kcal mol^{-1}, leading to the conclusion that the Mills–Nixon effect discriminates β- and α-positions by some 2–3 kcal mol^{-1} in the protonation process. The most basic spot in fluorene **24** is the C(4) atom because both the MN and the resonance effects act in a synergistic manner in that case.

Concluding remarks

It is found that the spatial structure of the parent biphenyl is well described by the semiempirical AM1 scheme. In particular, the dihedral twist angle φ is well reproduced being as large as 45°. It is a compromise between the conjugation interaction, which tends to diminish the dihedral angle and the steric hindrance caused by the proximity of four neighbouring H atoms. The hindered rotation potential is well described by the applied theoretical models. The scaled $(AM1)_{sc}$ model reproduces very well the proton affinity of this compound. Its *PA* value is some 13 kcal mol^{-1} larger than that of benzene because of the resonance effect and the concomitant favourable distribution of the positive charge over the whole system. The most basic site is given by the apical (*para*) carbon atom. The corresponding increase in the π-electron conjugation is reflected *inter alia* in a decrease of the twist angle by ~20° in the corresponding conjugate acid. It is noteworthy that *ipso* and *meta* proton affinities differ very little from the *PA* value of benzene due to an apparent lack of the resonance effect.

Table 5 The *PA* values of fluorene and indan as calculated by the $(AM1)_{sc}$ model (in kcal mol^{-1})[a]

Fluorene–H^+	*PA*	Indan–H^+	*PA*	*Δ*
$\mathbf{24_2}$	196.2	$\mathbf{25_2}$	189.1	7.1
$\mathbf{24_3}$	191.5	$\mathbf{25_3}$	191.9	−0.4
$\mathbf{24_4}$	198.9	$\mathbf{25_4}$	191.9	7.0
$\mathbf{24_5}$	188.6	$\mathbf{25_5}$	189.1	−0.5

[a] *Δ* is the difference between the corresponding *PA*s of fluorene and indan.

The proton affinities of the polysubstituted biphenyls involving F and CH_3 substituents follow very closely the additivity rule based on the independent substituent approximation (ISA). Variation in the *PA* of substituted biphenyls can be rationalized in qualitative terms by an interplay between the resonance and steric effects. The large *PA* values over 200 kcal mol^{-1} are found in **22**. Additional amplification of the basicity can be expected by properly positioned OCH_3 and NH_2 groups, which represent strong π-electron donating substituents.

Finally, the proton affinity of fluorene and the location of its most basic site were interpreted and indentified, respectively, by the synaction of the Mills–Nixon and resonance effects. The latter is a predominating factor.

References

1 R. W. Alder, P. S. Bowman, W. R. S. Steele and D. R. Winterman, *J. Chem. Soc., Chem. Commun.*, 1968, 723.
2 R. W. Alder, *Chem. Rev.*, 1989, **89**, 1215.
3 A. L. Llamas-Saiz, C. Foces-Foces and J. Elguero, *J. Mol. Struct.*, 1994, **328**, 297.
4 R. W. Alder, *Tetrahedron*, 1990, **46**, 683.
5 F. Hibbert and J. Emsley, *Adv. Phys. Org. Chem.*, 1990, **26**, 255.
6 R. Grigg, P. McMeekin and V. Sridharan, *Tetrahedron*, 1995, 13331.
7 K. Platteborze-Stienlet and T. Zeegers-Huyskens, *J. Mol. Struct.*, 1996, **378**, 29.
8 B. Brzezinski, E. Grech, Z. Malarski, M. Rospenk, G. Schroeder and L. Sobczyk, *J. Chem. Res.* (*S*), 1997, 151.
9 K. Wozniak, H. He, J. Klinowski, W. Jones and T. L. Barr, *J. Phys. Chem.*, 1995, **99**, 14667.
10 A. I. Gonzáles, O. Mó, M. Yañez, E. Léon, J. Tortajada, J. P. Morizur, I. Leito, P.-C. Maria and J. F. Gal, *J. Phys. Chem.*, 1996, 10490.
11 B. Amekraz, J. Tortajada, J. P. Morizur, A. I. Gonzáles, O. Mó, M. Yañez, I. Leito, P.-C. Maria and J. F. Gal, *New J. Chem.*, 1996, 1011.
12 M. J. Paräkylä, *J. Org. Chem.*, 1996, **61**, 7420.
13 A. Szemila-Hojniak, J. M. Zwier, W. J. Buma, R. Bursi and J. H. van der Waals, *J. Am. Chem. Soc.*, 1998, **120**, 4840.
14 E. Fujiwara, K. Omoto and H. Fujimoto, *J. Org. Chem.*, 1997, 7234.
15 R. A. Peerboom, S. Ingemann, N. M. M. Nibbering and J. F. Liebman, *J. Chem. Soc., Perkin Trans. 2*, 1990, 1825.
16 E. D. Raczynska and R. W. Taft, *Bull. Chem. Soc. Jpn.*, 1997, 1297.
17 E. D. Raczynska, P.-C. Maria, J.-F. Gal and M. Decouzon, *J. Phys. Org. Chem.*, 1994, **70**, 725.
18 B. Kovačević, Z. B. Maksić and P. Rademacher, *Chem. Phys. Lett.*, 1998, **293**, 245.
19 B. Kovačević and Z. B. Maksić, *Chem. Phys. Lett.*, 1998, **288**, 289.

20 Z. B. Maksić and B. Kovačević, *J. Phys. Chem. A*, 1998, **102**, 7324.
21 Z. B. Maksić and M. Eckert-Maksić, in *Theoretical Organic Chemistry*, C. Párkány, Ed., Elsevier, Amsterdam, 1998, p. 203 and references cited therein.
22 Z. B. Maksić, B. Kovačević and D. Kovaček, *J. Phys. Chem. A*, 1997, **101**, 7446 and references cited therein.
23 G.-P. Charbonneau and Y. Delugeord, *Acta Crystallogr.*, *Sect. B*, 1977, **33**, 1586.
24 O. Bastiansen and M. Traetteberg, *Tetrahedron*, 1962, **17**, 147; A. Almeningen, O. Bastiansen, L. Fernholt, B. N. Cyvin, S. J. Cyvin and S. Samdal, *J. Mol. Struct.*, 1985, **128**, 59; O. Bastiansen and S. Sandal, *J. Mol. Struct.*, 1985, **128**, 115.
25 H. Suzuki, *Bull. Chem. Soc. Jpn.*, 1959, **32**, 1340.
26 E. C. Lim and Y. H. Li, *J. Chem. Phys.*, 1970, **52**, 6416.
27 V. J. Eaton and D. Steele, *J. Chem. Soc.*, *Faraday Trans. 2*, 1973, **69**, 1601.
28 H. Uchimura, A. Tajiri and M. Hatano, *Chem. Phys. Lett.*, 1975, **34**, 34; *Bull. Chem. Soc. Jpn.*, 1981, **54**, 3279.
29 M. Akiyama, T. Watanabe and M. Kakihana, *J. Phys. Chem.*, 1986, **90**, 1752.
30 E. Hunter, NIST, private communication.
31 M. Eckert-Maksić, M. Klessinger and Z. B. Maksić, *Chem. Eur. J.*, 1996, **2**, 1251.
32 D. Kovaček, Z. B. Maksić and I. Novak, *J. Phys. Chem. A*, 1997, **101**, 1147.
33 M. Eckert-Maksić, M. Klessinger and Z. B. Maksić, *J. Phys. Org. Chem.*, 1997, **10**, 415.
34 Z. B. Maksić, M. Eckert-Maksić and M. Klessinger, *Chem. Phys. Lett.*, 1996, **26**, 572.
35 W. H. Mills and I. G. Nixon, *J. Chem. Soc.*, 1930, 2510.
36 Z. B. Maksić, M. Eckert-Maksić, M. Hodošček, W. Koch and D. Kovaček, in *Molecules in Natural Sciences and Medicine—An Encomium for Linus Pauling*, Z. B. Maksić and M. Eckert-Maksić, Ed., Ellis Horwood, Chichester, 1991, p. 333.
37 R. Rathore, S. V. Lindeman, A. S. Kumar and J. K. Kochi, *J. Am. Chem. Soc.*, 1998, **120**, 6012 and references cited therein.
38 M. Eckert-Maksić, Z. B. Maksić and M. Klessinger, *Int. J. Quantum Chem.*, 1994, **49**, 383.
39 M. Eckert-Maksić, Z. B. Maksić and M. Klessinger, *J. Chem. Soc.*, *Perkin Trans. 2*, 1994, 285.
40 M. Eckert-Maksić, M. Klessinger, D. Kovaček and Z. B. Maksić, *J. Phys. Org. Chem.*, 1996, **9**, 269.
41 H. C. Brown, J. H. Brewster and H. Schechter, *J. Am. Chem. Soc.*, 1954, **76**, 467.

Paper 8/08501C